THE JOURNAL OF PHYSICAL CHEMISTRY B LETTERS

2006, *110,* 5845−5848
Published on Web 03/08/2006

One-Pot Redox Syntheses of Heteronanostructures of Ag Nanoparticles on MoO_3 Nanofibers

Wenjun Dong,[†,‡] Zhan Shi,[†] Jingjing Ma,[†] Changmin Hou,[†] Qiang Wan,[†] Shouhua Feng,*[,†] Andrew Cogbill,[‡] and Z. Ryan Tian*[,‡]

State Key Laboratory of Inorganic Synthesis and Preparative Chemistry, College of Chemistry, Jilin University, Changchun 130012, P. R. China, and Department of Chemistry and Biochemistry, University of Arkansas, Fayetteville, Arkansas 72701

Received: January 20, 2006; In Final Form: February 17, 2006

A new one-pot redox route has been developed for simultaneous syntheses of Ag nanoparticles on MoO_3 nanofibers. Four different synthetic reactions that have been integrated into the one-pot synthesis include the oxidation of $[Na(H_2O)_2]_{0.25}MoO_3$ bronze, the reduction of silver ions, and the in situ simultaneous growth of the self-organized Ag nanoparticles and the MoO_3 nanofibers. This new strategy can be generally applicable to grafting various metal nanoparticles on nanofibers for new catalysis-related applications.

Synthesis of multifunctional one-dimensional (1D) nanostructures brings new hopes in fields of nanotechnology,[1] with novel synthetic methods and new 1-D nanomaterials being reported constantly.[2] On this basis, synthesis of multifunctional heteronanostructures from simple nanostructured building blocks has become a new challenge in nanomaterials research. Heteronanostructures, like tetrapod,[3] nanorods-on-nanoplates,[4] and nanoparticles-on-nanofibers,[5−8] have attracted much attention due to their unusual application potentials.

Mainly, two synthetic strategies have been reported to be successful in the syntheses of nanoparticles on nanofibers. One uses organics (e.g., supramolecules,[9] organic ligands,[10−12] and biomolecules[13−15]) for assisting the nucleation and growth of nanoparticles, and for preventing the nanoparticles from unwanted irreversible aggregations. The other involves physical and chemical depositions of nanoparticles on a variety of nanofibrous substrates including carbon nanotubes,[16−19] polymer nanofibers,[20] and TiO_2 nanofibers.[21] On this basis, synthesis of heteronanostructures by grafting catalytic metal nanoparticles on nanofibers could result in new nanotechnologies for catalysis, sensing, and battery applications.

Controlling the average oxidation state of molybdenum (Mo) in its oxide, between (V) and (VI), can provide the oxides with superb redox properties useful in the above-mentioned applications. Modifying the oxide 1D nanomaterial surface with metal nanoparticles would make these properties[22−30] optimally integrated into one heteronanostructure for making new catalysts, sensors, and battery electrodes. Here, we report for the first time a simple, simultaneous redox hydrothermal synthesis of a heteronanostructure, composed of Ag nanoparticles on MoO_3 nanofibers, under the help of neither organics nor substrate.

Four different synthetic reactions have been involved in this one-pot synthesis. They are an oxidation of $[Na(H_2O)_2]_{0.25}MoO_3$ layered bronze, a reduction of silver ions, a growth of self-organized Ag nanoparticles, and that of MoO_3 nanofibers. Before the synthesis, the $[Na(H_2O)_2]_{0.25}MoO_3$ bronze was made separately via a method reported in the literature[31] and then ion-exchanged with Ag^+ in water.

The entire synthesis is illustrated in Figure 1 and represented by reaction 1 and reaction 2. In the synthesis, 0.5 g $[Na(H_2O)_2]_{0.25}MoO_3$ was dispersed in 100 mL of 0.01 mol/L $AgNO_3$ solution, stirred for 30 min, and then aged at 0 °C in a nitrogen atmosphere for 5 h. This ion-exchange process (reaction 1) was repeated by three times to bring the process to completion. Thereafter, the precipitate was washed and then transferred into a Teflon-lined vessel containing 15 mL of 1.0 mol/L $AgNO_3$ solution. After a hydrothermal treatment at 150 °C for 1 h in an autoclave container (reaction 2), the light-gray powdery product was collected and then rinsed with deionized water, followed by a vacuum-dry at 100 °C for 5 h.

$$[Na(H_2O)_2]_{0.25}MoO_3 + Ag^+ \rightarrow [Ag(H_2O)_{1<x<2}]_{0.25}MoO_3 \quad (1)$$

$$[Ag(H_2O)_{1<x<2}]_{0.25}MoO_3 \rightarrow \text{Ag nanoparticles-on-}MoO_3\text{ nanofibers} \quad (2)$$

X-ray powder diffraction (XRD, Siemens D5005) studies have confirmed the completion of reactions 1 and 2. The XRD pattern of the $[Ag(H_2O)_{1<x<2}]_{0.25}MoO_3$ is similar to that of the $[Na(H_2O)_2]_{0.25}MoO_3$, suggesting a similar crystal structure for these two samples collected before and after the ion exchange. Results from inductively coupled plasma (ICP, Perkin-Elmer Optima 3300DV spectrometer) analysis for the $[Ag(H_2O)_{1<x<2}]_{0.25}MoO_3$ show that the Na wt % was lower than the detection limit. Results from the energy-dispersive X-ray analyses (EDX, FESEM, Philips ESEM XL30) reports that only Ag, Mo, and O elements were present in the $[Ag(H_2O)_{1<x<2}]_{0.25}MoO_3$, also

* Email addresses: shfeng@mail.jlu.edu.cn; rtian@uark.edu.
[†] State Key Laboratory of Inorganic Synthesis and Preparative Chemistry, Jilin University.
[‡] University of Arkansas.

10.1021/jp060437e CCC: $33.50

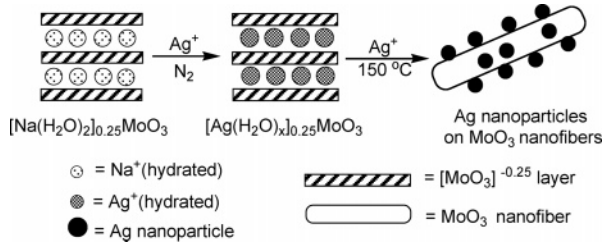

Figure 1. Schematic illustration of formation of the silver nanoparticles on the MoO_3 nanofibers.

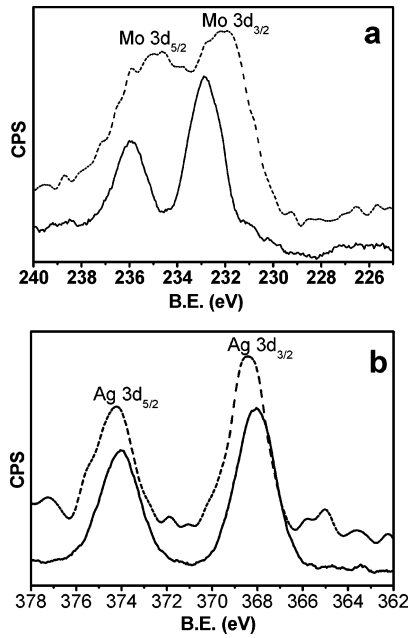

Figure 2. XPS spectra of Mo and Ag. (a) Mo in the final product of Ag-NP-MoO_3-NF (—) and $[Na(H_2O)_2]_{0.25}MoO_3$(- - -). (b) Ag in the Ag-NP-MoO_3-NF (—) and $[Ag(H_2O)_x]_{0.25}MoO_3$ (- - -).

suggesting that the ion-exchange process was almost complete. The XRD diffraction pattern of the Ag-nanoparticles-on-MoO_3-nanofibers (Ag-NP-MoO_3-NF) proves the existence of cubic Ag by its four characteristic peaks [$2\theta = 38.2°$ (111), 44.4° (200), 64.6° (220), and 77.6° (311), (JCPDS card no. 04-0783)] and the formation of the MoO_3-based nanofibers by the rest diffraction peaks.[22−24]

X-ray photoelectron spectroscopy (XPS, ESCALAB Mark II) was used to further confirm the redox reaction between the Ag and the Mo. The binding energies obtained in the XPS analysis were corrected for specimen charging by referencing the C1s to 284.60 eV. The XPS spectra of Mo in the product (Ag-NP-on-MoO_3-NF) and the starting material $(MoO_3)^{-0.25}$ are shown in Figure 2a. A peak shift of 1.4 eV of Mo $3d_{5/2}$ from the lower (234.6 eV) to the higher (236.0 eV) binding energies clearly indicates that an oxidization from $Mo^{5.75+}$ to Mo^{6+} took place during the autoclave treatment.[32] The XPS spectra of Ag $3d_{5/2}$ in $[Ag(H_2O)_x]_{0.25}MoO_3$ and Ag-NP-on-MoO_3-NF, however, showed a reduction from Ag^+ to Ag^0 due to an energy shift from 368.5 eV (Ag^+) to 368.1 eV (Ag^0), as shown in Figure 2b. This statement is supported by another fact that the Ag $3d_{5/2}$ peak at a binding energy of 368.1 eV with its fwhm of 1.9 eV has a splitting of the 3d doublet about ca. 6.0 eV. All the XPS experimental data are in a good agreement with what have been reported in the reference for both Ag^+ to Ag^0 and Mo^{5+} to Mo^{6+}, suggesting an oxidation state of (VI) for Mo and that of (0) for Ag in the final heteronanostructure.[32−34]

Morphologies of the final products of Ag-NP-MoO_3-NF were characterized by transmission electron microscopy (TEM, JEOL-3010). The products were first dispersed by sonication for 2−3 min in ethanol and then transferred onto a holey copper grid coated with carbon. The TEM images in Figure 3a,b have depicted that Ag nanoparticles were highly dispersed on the surface of the MoO_3 nanofibers. From these images, one can see that the Ag nanoparticles have quite uniformly scattered across the entire surface of the MoO_3 nanofibers. The diameter of the synthesized nanofibers falls in a relatively narrow range of 50−80 nm, and the length of the nanofibers ranges from several to tens of micrometers. The diameter of the Ag nanoparticle, grown on the MoO_3 nanofiber, is in the range 3−15 nm. A local HRTEM image in Figure 3c indicates that the Ag particles are nearly spherical, with a face-centered cubic lattice of the metallic silver that is in line with the XRD result. The EDX spectrum of this final product Ag-NP-MoO_3-NF (see Figure 3a) is depicted in Figure 3d for clearly showing the existence of Ag, Mo, and O in the final product.

As mentioned above, the growth of the Ag nanoparticles involves a redox reaction between the Ag (I) and the Mo (V). Each Mo (V) would likely serve as a redox center. If so, the original distribution of the Mo(V) in the layered structure would determine the initial population of the freshly reduced Ag^0. During the autoclave treatment, the migration of the reduced Ag to form the Ag nanoparticle was likely accompanied by the transformation from the layered structure to the nanofiber of MoO_3, resulting in the Ag nanoparticles self-organized across the entire surface of the nanofiber (as shown in Figure 3b). It has been reported in the literature that lamellar structures can be readily converted into nanofibers under hydrothermal conditions.[35] A further detailed work on the understanding of the mechanisms, involving such a simultaneous redox synthesis of two different nanostructures, is currently underway to further understand the quality of the Ag nanoparticles.[36,37]

The size and the population density of the Ag nanoparticles can be systematically controlled by the $AgNO_3$ concentration in the hydrothermal treatment. Figure 4a,b show TEM images of the Ag-NP-MoO_3-NF from a hydrothermal treatment in a 5.0 mol/L $AgNO_3$ solution at 150 °C for 60 min. The Ag nanoparticles formed at this concentration had diameters ranging from 8 to 18 nm and covered nearly 55% of the surface on each MoO_3 nanofiber. When the concentration of $AgNO_3$ was reduced to 0.10 mol/L (see Figure 4c,d), the Ag nanoparticles would have a diameter range of 4−10 nm and cover about 15% of the MoO_3 nanofiber surface, as shown in Figure 4d. Results of Figure 3a,b (1.0 mol/L $AgNO_3$) and Figure 4 have demonstrated our controls over the average size of the Ag nanoparticles from 7 to 10 nm and then to 13 nm, with their population densities on the MoO_3 nanofibers from ∼15% to ∼40% and then to ∼55%, respectively. The similar self-organization along the nanofiber axis, shown in Figure 4b,d, appeared to not be as organized as in the case of Figure 3b, showing the concentration effect on the size and spatial organization of the nanoparticle in a confined environment within a narrow synthetic window.

The Ag−MoO_3, like the Au nanoparticles over TiO_2, has shown superb properties.[26−30] The investigations of Au nanoparticles over TiO_2 have revealed that deposition of catalytic metal on catalytic metal oxide improves the overall efficiency of redox photocatalysis due probably to the enhanced interfacial charge transfer.[38,39] Likewise, anchoring the catalytic Ag nanoparticles on the MoO_3 nanowire catalyst could result in an improved overall photocatalytic efficiency.

The photocatalytic properties of the Ag-NP-MoO_3-NF were studied at room temperature (RT) in aqueous solutions containing $(C_2H_5O)_2P(O)(H_2CSC_6H_5)$ (Alfa-Aesar) that is a nerve agent

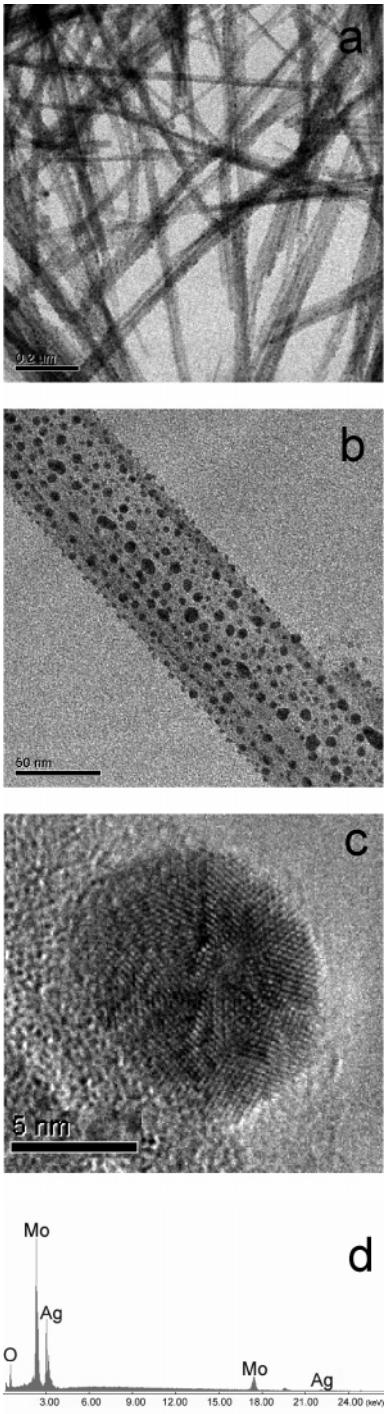

Figure 3. TEM images of the final product of Ag-NP-MoO_3-NF: (a) a low-magnification image showing the yield and purity of the final product; (b) a high-magnification image showing the nanoparticles self-organized on the nanofibers; (c) an HRTEM lattice image of a Ag nanoparticle on a MoO_3 nanofiber; d) an EDX spectrum of Ag-NP-MoO_3-NF.

simulant (NAS). The NAS solution was made by dissolving 10 μL of the NAS and 1 mL ethanol into 100 mL water, into which 10 mg of the 10 nm Ag-NP-MoO_3-NF was added. The UV illumination from the lamp (Mineralight UVGL-58, $\lambda = 254$ nm) was about 5 mm above the solution, and the NAS concentration was measured using the UV−visible spectrometer (HP 8453). After a 45 min UV illumination, the NAS concentration was reduced by 41%. A blank test using the Ag-NP-MoO_3-NF of same weight without the UV illumination shows that the NAS concentration was decreased by only 2%, which

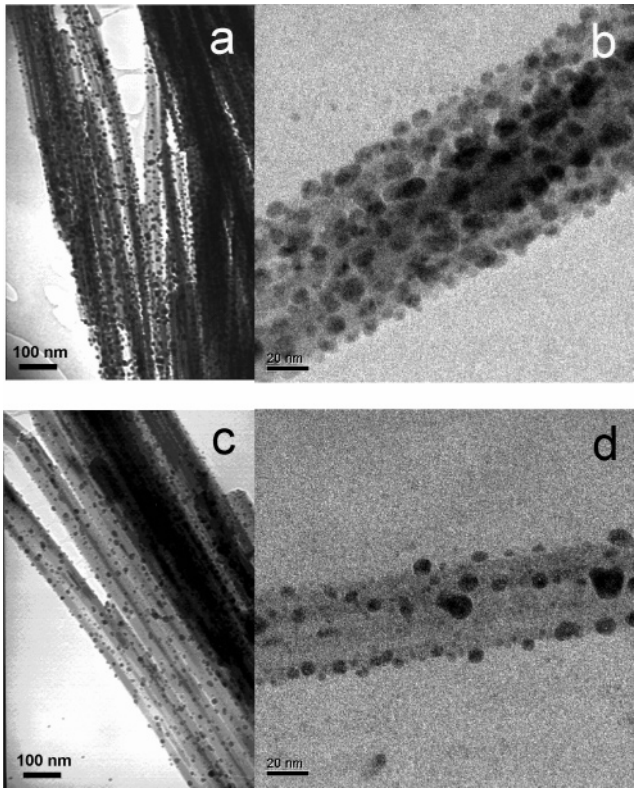

Figure 4. TEM images of the silver nanoparticles on MoO_3 nanofibers: (a) a low-magnification image and (b) a high-magnification image of the final product from the 5.0 mol/L of $AgNO_3$; (c) a low-magnification image and (d) a high-magnification image of the final product from the 0.1 mol/L of $AgNO_3$.

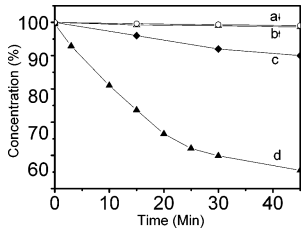

Figure 5. The plot of the NAS concentration change vs time from different catalysts: (a) MoO_3 nanofibers with the UV irradiation, and the average diameter of the MoO_3 nanofibers is 100 nm; (b) Ag-NP-MoO_3-NF (10 nm Ag) without the UV irradiation; (c) anatase TiO_2 particles with the same UV irradiation; (d) Ag-NP-MoO_3-NF (10 nm Ag) with the same UV irradiation. (Absorbance was measured at 251 nm).

suggests that the 41% concentration drop was mainly due to the photocatalytic decomposition rather than a surface adsorption on the Ag nanoparticle and/or MoO_3 nanofiber. Under the same condition, MoO_3 nanofibers (prepared by another method[24] to have an average diameter of 100 nm) and anatase TiO_2 powder (325 mesh, Alfa-Aesar) of the same weight were used to photocatalytically decompose the NAS, resulting in drop of the NAS concentrations by 1% and 10%, respectively. All these catalytic results were clearly illustrated in Figure 5. During the reaction, no change in the solution temperature was observed after the UV radiation in this work. Likely, this preliminary catalytic conversion could be further improved by optimizations of the time and intensity of the UV radiation, the reaction temperature, and the catalyst structure and morphology. To our knowledge, this 41% conversion represents a very efficient photocatalytic decomposition of NAS in water at RT.[40,41] Our further detailed work on controlling the weight, structure, and size dispersion of Ag nanoparticles on MoO_3 nanofibers might

lead to the development of new catalysts for a variety of important catalysis-related applications.

In summary, this simple one-pot redox synthesis of Ag-NP-MoO_3-NF could be among the first for synthesis of heteronanostructures in a one-step treatment. On this basis, the surface properties of these heteronanostructures can be fine-tuned by controlling the nature of the grafted metal nanoparticles for obtaining better catalytic properties. This work would shed new light on the development of new nanomaterials for important applications in catalysis.

Acknowledgment. This work was supported by the National Natural Science Foundation of China. W.D. and Z.R.T. highly appreciate the financial supports from the University of Arkansas and Dr. N. Pradhan and Prof. X. Peng for their help on the UV−vis work.

References and Notes

(1) Xia, Y.; Yang, P.; Sun, Y.; Wu, Y.; Mayers, B.; Gates, B.; Yin, Y.; Kim, F.; Yan, H. *Adv. Mater.* **2003**, *15*, 353.

(2) Burda, C.; Chen, X.; Narayanan, R.; El-Sayed, M. A. *Chem. Rev.* **2005**, *105*, 1025.

(3) Milliron, D. J.; Hughes, S. M.; Cui, Y.; Manna, L.; Li, J.; Wang, L.-W.; Alivisatos, A. P. *Nature (London)* **2004**, *430*, 190.

(4) Tian, Z. R.; Voigt, J. A.; Liu, J.; McKenzie, B.; McDermott, M. J.; Rodriguez, M. A.; Konishi, H.; Xu, H. *Nat. Mater.* **2003**, *2*, 821.

(5) Choi, H. C.; Shim, M.; Bangsaruntip, S.; Dai, H. *J. Am. Chem. Soc.* **2002**, *124*, 9058.

(6) Zamborini, F. P.; Leopold, M. C.; Hicks, J. F.; Kulesza, P. J.; Malik, M. A.; Murray, R. W. *J. Am. Chem. Soc.* **2002**, *124*, 8958.

(7) Luo, J.; Jones, V. W.; Maye, M. M.; Han, L.; Kariuki, N. N.; Zhong, C. J. *J. Am. Chem. Soc.* **2002**, *124*, 13988.

(8) Kim, H.-S.; Lee, H.; Han, K.-S.; Kim, J.-H.; Song, M.-S.; Park, M.-S.; Lee, J.-Y.; Kang, J.-K. *J. Phys. Chem. B* **2005**, *109*, 8983.

(9) Jiang, K.; Eitan, A.; Schadler, L. S.; Ajayan, P. M.; Siegel, R. W.; Robert, N.; Mayne, M.; Reyes-Reyes, M.; Terrones, H.; Terrones, M. *Nano Lett.* **2003**, *3*, 275.

(10) Han, L.; Wu, W.; Kirk, F. L.; Luo, J.; Maye, M. M.; Kariuki, N. N.; Lin, Y.; Wang, C.; Zhong, C.-J. *Langmuir* **2004**, *20*, 6019.

(11) Ellis, A. V.; Vijayamohanan, K.; Goswami, R.; Chakrapani, N.; Ramanathan, L. S.; Ajayan, P. M.; Ramanath, G. *Nano Lett.* **2003**, *3*, 279.

(12) Zhang, J.; Wang, G.; Shon, Y. S.; Zhou, O.; Superfine, R.; Murray, R. W. *J. Phys. Chem. B* **2003**, *107*, 3726.

(13) Lee, S. W.; Mao, C. B.; Flynn, C. E.; Belcher, A. M. *Science* **2002**, *296*, 892.

(14) Shenton, W.; Douglas, T.; Young, M.; Stubbs, G.; Mann, S. *Adv. Mater.* **1999**, *11*, 253.

(15) Behrens, S.; Rahn, K.; Habicht, W.; Bohm, K.-J.; Rosner, H.; Dinjus, E.; Unger, E. *Adv. Mater.* **2002**, *14*, 1621.

(16) Day, T. M.; Unwin, P. R.; Wilson, N. R.; MacPherson, J. V. *J. Am. Chem. Soc.* **2005**, *127*, 10639.

(17) Quinn, B. M.; Dekker, C.; Lemay, S. G. *J Am. Chem. Soc.* **2005**, *127*, 6146.

(18) Lin, Y.; Cui, X.; Yen, C.; Wai, C. M. *J. Phys. Chem. B* **2005**, *109*, 14410.

(19) Qu, L.; Dai, L. *J. Am. Chem. Soc.* **2005**, *127*, 10806.

(20) Guo, Y.-G.; Hu, J.-S.; Liang, H.-P.; Wan, L.-J.; Bai, C.-L. *Chem. Mater.* **2003**, *15*, 4332.

(21) Wen, B.; Liu, C.; Liu, Y. *J. Phys. Chem. B* **2005**, *109*, 12372.

(22) Niederberger, M.; Krumeich, F.; Muhr, H.-J.; Muller, M.; Nesper, R. *J. Mater. Chem.* **2001**, *11*, 1941.

(23) Lou, X. W.; Zeng, H. C. *Chem. Mater.* **2002**, *14*, 4781.

(24) Michailovski, A.; Grunwaldt, J.-D.; Baiker, A.; Kiebach, R.; Bensch, W.; Patzke, G. R. *Angew. Chem., Int. Ed.* **2005**, *44*, 5643.

(25) Wei, X. M.; Zeng, H. C. *J. Phys. Chem. B* **2003**, *107*, 2619.

(26) Lou, X. W.; Zeng, H. C. *J. Am. Chem. Soc.* **2003**, *125*, 2697.

(27) Dong, W.; Feng, S.; Shi, Z.; Li, L.; Xu, Y. *Chem. Mater.* **2003**, *15*, 1941.

(28) Uchijima, F.; Takagi, T.; Itoh, H.; Matsuda, T.; Takahashi, N. *Phys. Chem. Chem. Phys.* **2000**, *2*, 1077.

(29) Takeshi, M.; Ayako, H.; Fumiko, U.; Hirotoshi, S.; Nobuo, T. *Microporous Mesoporous Mater.* **2002**, *51*, 155.

(30) Noh, H.; Wang, D.; Luo, S.; Flanagan, T. B.; Balasubramaniam, R.; Sakamoto, Y. *J. Phys. Chem. B* **2004**, *108*, 310.

(31) Thomas, D. M.; McCarron, E. M., III. *Mater. Res. Bull.* **1986**, *21*, 945.

(32) Briggs, D., Seah, M. P., Eds. *Practical Surface Analysis*; John Wiley and Sons: New York, 1983.

(33) Srnova-Sloufova, I.; Vlckova, B.; Bastl, Z.; Hasslett, T. L. *Langmuir* **2004**, *20*, 3407.

(34) He, J.; Ichinose, I.; Kunitake, T.; Nakao, A.; Shiraishi, Y.; Toshima, N. *J. Am. Chem. Soc.* **2003**, *125*, 11034.

(35) Wang, J.; Li, Y. *Adv. Mater.* **2003**, *15*, 445.

(36) Correa-Duarte, M. A.; Sobal, N.; Liz-Marzán, M. L.; Giersig, M. *Adv. Mater.* **2004**, *16*, 2179.

(37) Grzelczak, M.; Correa-Duarte, M. A.; Salgueiriño-Maceira, V.; Giersig, M.; Diaz, R.; Liz-Marzán, L. M. *Adv. Mater.* **2006**, *18*, 415.

(38) Subramanian, V.; Wolf, E. E.; Kamat, P. V. *J. Am. Chem. Soc.* **2004**, *126*, 4943.

(39) Yan, W.; Mahurin, S. M.; Pan, Z.; Overbury, S. H. Dai, S. *J. Am. Chem. Soc.* **2005**, *127*, 10480.

(40) Moss, J. A.; Szczepankiewicz, S. H.; Park, E.; Hoffmann, M. R. *J. Phys. Chem.* B **2005**, *109*, 19779.

(41) Segal, S. R.; Suib, S. L. *Chem. Mater.* **1999**, *11*, 1687.